BIOCHEMISTRY
including biophysical chemistry & molecular biology

ARTICLE

pubs.acs.org/biochemistry

Biophysical Investigation of the Iron in Aft1-1^{up} and Gal-YAH1 *Saccharomyces cerevisiae*

Ren Miao,[†] Gregory P. Holmes-Hampton,[†] and Paul A. Lindahl*[,†,‡]

[†]Department of Chemistry, Texas A&M University, College Station, Texas 77843-3255, United States

[‡]Department of Biochemistry and Biophysics, Texas A&M University, College Station, Texas 77843-2128, United States

Supporting Information

ABSTRACT: Aft1p is a major iron regulator in budding yeast *Saccharomyces cerevisiae*. It indirectly senses cytosolic Fe status and responds by activating or repressing iron regulon genes. Aft1p within the Aft1-1^{up} strain has a single amino acid mutation which causes it to constitutively activate iron regulon genes regardless of cellular Fe status. This leads to elevated Fe uptake under both low and high Fe growth conditions. Ferredoxin Yah1p is involved in Fe/S cluster assembly, and Aft1p-targeted iron regulon genes are also upregulated in Yah1p-depleted cells. In this study Mössbauer, EPR, and UV−vis spectroscopies were used to characterize the Fe distribution in Aft1-1^{up} and Yah1p-depleted cells. Aft1-1^{up} cells grown in low Fe medium contained more Fe than did WT cells. A basal level of Fe in both WT and Aft1-1^{up} cells was located in mitochondria, primarily in the form of Fe/S clusters and heme centers. The additional Fe in Aft1-1^{up} cells was present as mononuclear HS Fe(III) species. These species are in a nonmitochondrial location, assumed here to be vacuolar. Aft1-1^{up} cells grown in high Fe medium contained far more Fe than found in WT cells. The extra Fe was present as HS Fe(III) ions, probably stored in vacuoles, and as Fe(III) phosphate nanoparticles, located in mitochondria. Yah1p-deficent cells also accumulated nanoparticles in their mitochondria, but they did not contain HS Fe(III) species. Results are interpreted by a proposed model involving three homeostatic regulatory systems, including the Aft1 system, a vacuolar iron regulatory system, and a mitochondrial Fe regulatory system.

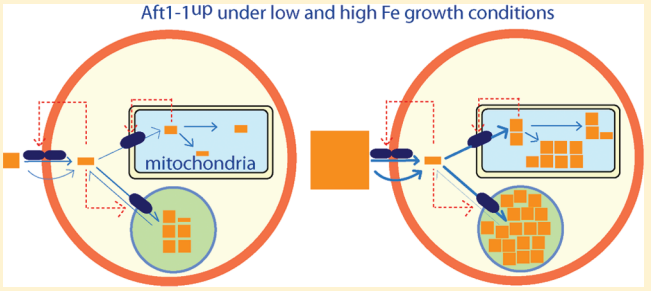

Iron is involved in many aspects of cellular metabolism, including respiration and catalysis.[1] However, this transition metal can also promote deleterious reactions that produce reactive oxygen species (ROS). Therefore, cellular trafficking and regulation of Fe are especially important. Iron trafficking begins with the influx of Fe from the growth medium into the cytosol via transporters in the plasma membrane.[2] The majority of these imported ions enter vacuoles and mitochondria, Fe "traffic hubs" that store Fe and house Fe-rich respiratory complexes, respectively. The nucleus regulates traffic by controlling expression of genes that encode membrane-bound Fe transporters as well as other proteins involved in Fe regulation and trafficking.

In budding yeast *Sacchromyces cerevisiae*, the dominant Fe import pathway under regular aerobic growth conditions involves the plasma membrane proteins Fet3p and Ftr1p. These proteins form a ferroxidase−permease complex that imports Fe with high affinity.[3] Once in the cytosol, Fe is sensed indirectly by Aft1p and perhaps Aft2p, transcription factors that control expression of FET3, FTR1, and ∼20 other genes collectively known as the *iron regulon*.[4] Aft1p moves between the cytosol and the nucleus in an iron-dependent manner. When cytosolic Fe levels are low, Aft1p localizes predominantly in the nucleus where it binds the promoter region of iron regulon genes and activates their expression. With high cytosolic Fe levels, Aft1p exits the nucleus, and expression of the iron regulon genes decline.[5] When grown on Fe-deficient medium (achieved by adding BPS), Δ*aft1* cells grow more poorly relative to WT cells due to their inability to uptake Fe from the medium.[6] Both cell types grow normally with high Fe concentrations in the medium.

Mitochondria are the primary cellular sites of Fe/S cluster (ISC) assembly and heme biosynthesis. Cytosolic ferrous ions enter mitochondria through the high-affinity transporters Mrs3/4p located on the inner membrane (IM). A pool of nonheme HS Fe(II) species in the mitochondria may be used as feedstock for ISC assembly and heme biosynthesis.[7] Iron transfers to ISC scaffold proteins. The ferredoxin Yah1p donates electrons required for ISC biosynthesis while the yeast frataxin homologue Yfh1p may donate Fe or activate ISC assembly.[8−10] The IM protein Atm1p exports an unknown species thought to be involved in cytosolic ISC biosynthesis. Deletion of these and other ISC-related proteins affords a common phenotype characterized by a respiration defect, the constitutive activation of iron regulon genes, the accumulation of Fe(III)

Received: December 18, 2010
Revised: January 29, 2011
Published: February 28, 2011

phosphate nanoparticles in mitochondria, and increased levels of ROS.[11−13]

Vacuoles are the major site of cellular Fe storage. Ccc1p is the only known vacuolar iron importer[14] while Fth1p and Smf3p are vacuolar membrane proteins that export Fe into the cytosol.[3] Kosman et al. have proposed that vacuolar Fe is in the Fe(III) state,[15] and this is supported by our previous observations.[7]

Mitochondria and vacuoles appear to import Fe from a common cytosolic pool, and the concentration of this Fe pool appears to be related to the concentration of Fe in growth media. Thus, Δ*Δmrs3/4* cells exhibit a growth defect in Fe-deficient medium but grow normally on Fe-replete medium. Conversely, Δ*ccc1* cells grow normally in Fe-deficient medium but show a growth defect on high-iron medium.[14] Ccc1p-deficient vacuoles may be unable to import cytosolic Fe, and the excess cytosolic Fe inhibits cell growth, perhaps via ROS damage.[16] Toxicity can be suppressed by overproducing Mrs3/4p,[16] perhaps because this allows excess Fe_{cyt} to be imported into the mitochondria which somehow detoxifies it.

The cytosolic Fe pool is also feedstock for the nanoparticles that accumulate in mitochondria of ISC mutants. However, no accumulation occurs (and there is no respiratory defect) in ISC mutant cells in which *mrs3/4* is also deleted,[17] implying that this Fe enters via Mrs3/4p. Overexpressing Ccc1p also prevents Fe accumulation.[18]

Mitochondria and vacuoles interact functionally. In Δ*Δmrs3/4* cells, mitochondria are deficient in Fe and have reduced ISC and heme levels, and reduced aconitase activity, perhaps due to an inability to import sufficient Fe into the organelle.[19] Meanwhile, the vacuolar Fe level is increased, via activation of Ccc1p, so as to store Fe that would otherwise be in the cytosol. The activation of Ccc1p may reduce cytosolic Fe levels and thus activate Aft1p.[18] Aconitase activities are recovered when Ccc1p is deleted, again implying that vacuoles and mitochondria draw from a common pool of cytosolic Fe.

The Aft1-1^{up} strain has a mutation in Aft1p (C291F) that causes it to remain in the nucleus and constitutively activate Aft1p-controlled iron regulon genes, regardless of the Fe status of the medium. This stimulates the uptake of Fe regardless of the medium Fe concentration. Aft1-1^{up} cells cultivated in rich medium (with high Fe) contain higher than WT Fe levels.[20] Mutant cells with ISC defects (e.g., Yah1p-depleted cells) also have elevated Fe levels. This is thought to be due to the upregulation of the iron regulon.

In this study, we use biophysics to examine the cellular Fe in Aft1-1^{up} strains and to compare it to that in WT and Yah1p-depleted cells. Our results show that Aft1-dependent activation of the iron regulon increases the iron content of the cell and distributes that extra Fe primarily into HS Fe(III) species that are probably located in vacuoles. Some Fe is sent to the mitochondria where it is converted into Fe(III) (phosphate)[a] nanoparticles. In contrast, disruption of the ISC biosynthesis pathway by Yah1p depletion caused loss of what appears to be vacuolar iron and massive import of Fe in the mitochondria. We conclude that vacuolar and mitochondrial Fe are regulated by systems besides Aft1.

EXPERIMENTAL PROCEDURES

Yeast Strains and Media. Strain Aft1-1^{up} (*MATα, trp1-63, leu2-3,112, gcn4-101, his3-609, FRE1-HIS3::URA3, AFT1-1^{up}*), described in ref 6, was a generous gift from Dr. Jerry Kaplan (University of Utah). Strain Gal-YAH1 (*MATα, ura3-1, ade2-1, trp1-1, his3-11,15, leu2-3,112*), described in ref 21, was a generous gift from Dr. Roland Lill (Philipps-Universität, Marburg, Germany). Strain Aft2-1^{up} (*MATα, his3Δ1, leu2Δ0, ura3Δ0, his::AFT2-1^{up}, aft1::kanMX4*), described in ref 22, was a generous gift from Dr. Dennis Winge (University of Utah). W303 (*MATα, ura3-1, ade2-1, trp1-1, his3-11,15, leu2−3,112*) served as the wild-type (WT) control strain for Gal-YAH1 and Aft1-1^{up}. W303 is the true control for Gal-YAH1 but not for Aft1-1^{up}. It would have been more accurate to have used the true control for Aft1-1^{up}, but it was not in our possession. A Mössbauer spectrum for the true control of Aft2-1^{up} (BY4741) was obtained; it was indistinguishable from the corresponding W303 spectrum.

Aft1-1^{up}, Aft2-1^{up}, and W303 were maintained on YPAD (standard rich medium containing glucose (2% w/v) and 40 mg/L adenine sulfate) agar plates. Gal-YAH1 was maintained on YPAGal plates (same as YPAD except galactose was used as the carbon source). Typically, one colony was used to inoculate liquid medium. Complete minimal medium containing glucose (2% w/v) was used for liquid cell growth. Complete supplement mixture (MPBio) provided amino acids. To enrich cells with ^{57}Fe, a modified yeast nitrogen base (MPBio) which lacks copper and iron salts was used. Copper and iron were added back as copper sulfate (10 μM final concentration) and ^{57}Fe(III) citrate (various concentrations; see below). Standard rich medium containing (2%, w/v) glucose (YPD) was also used in some experiments.

Cell Growth, Harvesting, and Whole-Cell Sample Preparation. Cells were grown in 250 mL culture flasks to OD (600 nm) ∼ 1 (typically 16−20 h growth, 1 cm path length cuvette) and harvested by centrifugation. Harvested cells were washed with deionized H_2O, then with 100 μM EDTA (pH ∼8), and then again with deionized H_2O. To prepare Mössbauer and EPR samples, washed cells were packed by centrifugation into Mössbauer cups or custom-designed EPR tubes[23] at 6000*g* for 10 min. For mitochondrial isolation, cells were grown to an OD (600 nm) of ∼1 in a 25 L glass fermenter at 30 °C as described.[23] Mitochondria were isolated by density-gradient centrifugation, packed into EPR tubes and Mössbauer cups, and immediately frozen in liquid N_2 as described.[23]

RNA Extraction and Real-Time PCR. Aft1-1^{up} and WT (W303) cells were grown to OD (600 nm) 3.0−3.5 in complete minimal medium lacking iron and copper. Cells were harvested by centrifugation, diluted into fresh medium, and grown for an additional 4 h. The fresh medium contained either 100 μM BPS (iron deficient) or 10 μM copper sulfate and 40 μM Fe(III) citrate (iron rich). Cells were again harvested, then washed once with ice-cold deionized water, and frozen in liquid N_2 for future RNA extraction.

Total RNA was extracted using the hot-phenol method.[24] Briefly, thawed cells were resuspended in AE buffer (50 mM sodium acetate, pH 5.3, 10 mM EDTA). Cells were lysed by adding SDS (1% (w/v) final concentration) and an equal volume of AE buffer-equilibrated phenol. The mixture was incubated at 65 °C and vortexed briefly once every minute for 10 min. After incubation, the mixture was rapidly chilled in a dry ice/ethanol bath and centrifuged at the maximum speed using a Qualitron DW-41microcentrifuge (maximum speed 6400 rpm) at room temperature for 5 min. The aqueous phase was extracted with an equal volume of phenol/chloroform/isoamyl alcohol (volume ratio 25:24:1), followed by centrifugation. The aqueous phase was extracted with an equal volume of chloroform/isoamyl alcohol (volume ratio 24:1), followed by centrifugation. To the resulting aqueous phase was added 0.3 M sodium acetate, pH 5.3,

after which 2.5 volumes of ethanol were added to precipitate the RNA contained in that phase. After being washed with 80% ethanol, the RNA was air-dried, resuspended in sterile water, and kept frozen at −80 °C until use. The total yield of RNA was quantified at OD (260 nm). Contaminating DNA was removed by treating the RNA with DNA-Free reagent (Ambion) following the manufacturer's instructions. RNA integrity was confirmed using a 1% agarose gel and a Bioanalyzer (Agilent). Super Script Vilo cDNA synthesis kit (Applied Biosystems) was used to synthesize cDNA from RNA. qRT PCR was carried out on the synthesized cDNA using an ABI 7900 Real Time PCR machine (Applied Biosystems). Samples were prepared using Power SYBR green PCR master mix (Applied Biosystems) and primer pairs designed for specific genes (see Supporting Information Table S1 for the primer pairs used in this study).

Analytical Characterizations. Crude mitochondria were isolated according to published procedures.[21] Mitochondrial proteins were separated by SDS−PAGE and transferred to a polyvinylidene fluoride membrane (Bio-Rad). Yah1p antisera were used to detect Yah1p. Porin was detected using porin antisera as a loading control. Mitochondrial protein concentrations were determined using the Bradford protein assay kit (Pierce) following the manufacturer's instructions. Mitochondrial or whole-cell total iron concentrations were determined after digestion in nitric acid by ICP-MS or by the bathophenanthroline-sulfonate (BPS; Sigma) method.[11] Reported values refer to packed mitochondria or whole-cell condition adjusted for buffer void volume. Aconitase assays were performed essentially as described[11] by monitoring disappearance of *cis*-aconitate (Sigma) at 240 nm.

Fluorescent Determination of Interstitial Buffer Volume. The fraction of mitochondrial pellet volumes (V_{pellet}) due to buffer was determined using the cell-impermeable fluorescent Compound 5,[25] a generous gift from Dr. Kevin Burgess (Texas A&M University). Initially, cells were grown to an OD (600 nm) ∼ 1.2 and rinsed three times with 100 μM EDTA and then three times with deionized water. Resulting cells were packed (4000*g* for 5 min) into EPR tubes. The height of the pellet was marked on the tube, allowing V_{pellet} to be calculated from the mass of an equivalent volume of water. Pelleted cells were then resuspended in 200 μL of phosphate-buffered saline (PBS = 137 mM NaCl, 2.7 mM KCl, 10 mM Na_2HPO_4, 1.8 mM KH_2PO_4, pH 7.4) containing known concentrations of Compound 5. Cells were pelleted, and the supernatant was collected. The cells were resuspended in 200 μL of PBS without Compound 5 and pelleted; the supernatant was again collected. This process was repeated three times for each sample. The concentrations of Compound 5 in supernatant fractions were determined using a fluorescence spectrometer (Koala 90080; ISS Inc.). The volume of buffer (V_{buffer}) contributing to V_{pellet} was determined as described,[26] allowing the mitochondrial packing efficiency ($V_{pellet} - V_{buffer}/V_{pellet} \times 100$) to be calculated.

Spectroscopy. UV−vis spectroscopic analyses of mitochondria were performed using a Hitachi Model U3310 with a Head-On photomultiplier tube as described.[11] A suspension of purified mitochondria in 0.6 M sorbitol and 20 mM HEPES, pH 7.4, was solubilized in 200 μL of buffer containing 50 mM Tris, pH 8.0, 100 mM NaCl, and 1% (w/v) sodium deoxycholate. The resulting solution had a mitochondrial protein concentration of 4 mg/mL. Potassium ferricyanide (Acros Organics) and sodium dithionite (Sigma) were used respectively to oxidize and reduce cytochromes. Mössbauer spectra were collected on a Model MS4 WRC spectrometer (SEE Co., Edina, MN) that had been calibrated using α-Fe foil as described.[11] EPR spectra were collected on an X-band EMX spectrometer (Bruker Biospin, Billerica, MA) as described.[11]

Table 1. Quantification of mRNA Levels of Different Genes under Iron-Replete (Iron-Free Minimal Medium Supplemented with 40 μM Fe(III) Citrate) or Iron-Depleted (Iron-Free Minimal Medium Supplemented with 100 μM BPS) Conditions[a]

	mean Ct			
gene	WT + BPS	WT − BPS	Aft1-1^{up} + BPS	Aft1-1^{up} − BPS
FET3	17.4	22.6	16.9	16.5
FRE1	19.4	25.0	19.8	21.5
ACT1	17.9	17.0	17.6	17.1

[a] Ct indicates the cycles required to reach the fluorescence intensity threshold. ACT1 (actin) is a control.

RESULTS

Characterization of Aft1-1^{up}. Iron regulon genes, including FET3 and FRE1, should be strongly induced in WT cells grown under Fe-deficient conditions but not under Fe-replete conditions. This behavior was verified using quantitative RT-PCR. Under an Fe-deficient condition (with BPS in the medium), FET3 and FRE1 mRNA levels in WT cells were 30−50-fold higher than under an Fe-replete condition (with 40 μM Fe in the medium) (Table 1). In contrast, Aft1-1^{up} cells under both conditions afforded FET3 and FRE1 mRNA levels similar to those of WT cells under the Fe-deficient condition. These results confirm that the iron regulon genes in the Aft1-1^{up} cells used were constitutively activated regardless of Fe_{medium} concentration. This is consistent with the reported behavior of the Aft1-1^{up} strain[6], and it verifies the genotype of the cells used in this study.

Aft1-1^{up} cells were grown in Fe-deficient minimal medium supplemented with 1, 5, 40, and 500 μM ^{57}Fe. The medium endogenously contained 3−7 μM natural-abundance Fe, only a portion of which may be useable by the cell. The overall cellular Fe concentration increased with [Fe_{medium}] (Table 2). The tabulated values are Fe concentrations in packed cell pellets after adjusting for the contribution of the buffer void volume.

At the lowest [Fe_{medium}] tested (endogenous Fe plus 1 μM ^{57}Fe), the Fe concentration of WT cells was nearly 3-fold lower than in Aft1-1^{up} cells[7] (Table 2). Assuming that the expression level of the iron regulon in Aft1-1^{up} cells is maximal and that the difference in Fe content between the two cell types was due exclusively to Aft1-dependent processes, this result suggests that the expression level of the iron regulon in WT cells grown under these low Fe conditions was about one-third of maximal.

The Fe concentration of WT cells grown in medium supplemented with 40 μM ^{57}Fe was ∼6-fold lower than that in Aft1-1^{up} cells while the FET3 and FRE1 mRNA levels were repressed more than 70-fold. Aft1-1^{up} cells accumulated Fe due to the constitutive activation of the iron regulon. In WT cells grown under similar Fe conditions, the Aft1-dependent iron regulon system has been reported to be repressed,[6] and our results confirm this. The more modest fold difference in Fe concentrations between cell types compared to the more dramatic fold difference in FET3 and FRE1 mRNA levels suggests that an Aft1-independent import mechanism operates in cells grown with 40

Table 2. Characterization of Aft1-1^{up} Whole Cells and Isolated Mitochondria[a]

[^{57}Fe] added to growth medium (μM)	1	5	40	500
[Fe] in whole-cell sample (μM)	680 ± 30 (WT = 250 ± 80)	2300 ± 270	2800 ± 470 (WT = 440 ± 40)	3400 ± 410
[Fe] in isolated mitochondria (μM)	1400 ± 60	ND	8100 ± 520 (WT ~ 750)	ND
[protein] in isolated mitochondria (mg/mL)	71 ± 6	ND	84 ± 8	ND
aconitase activity[b]	480	ND	150	ND

[a] The volume contribution of the interstitial buffer was removed during calculation of tabulated values. The cells themselves occupied 70% of V_{pellet} (Supporting Information Table S2) in packed whole-cell samples. In packed mitochondria samples, mitochondria occupied 77% of V_{pellet}.[26] Comparative WT values are given in parentheses. [b] Aconitase activity was measured using purified mitochondria; relative error was estimated at ±20% ($n \geq 2$).

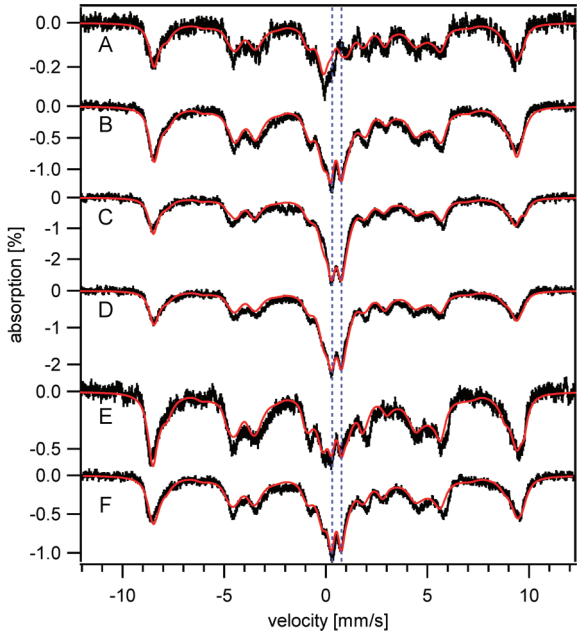

Figure 1. Mössbauer spectra of Aft1-1^{up} cells grown under various conditions. Spectra were collected at 6 K with 400 G magnetic field applied parallel to the γ-rays. (A−D) Cells grown on complete minimal medium containing 1, 5, 40, and 500 μM ^{57}Fe(III) citrate, respectively. (E, F) Cells grown on YPD medium containing 20 and 400 μM ^{57}Fe(III) citrate, respectively. Red lines are simulations assuming the species and percentages listed in Table 3. Blue dashed lines indicate the doublet positions of Fe(III) phosphate nanoparticles.

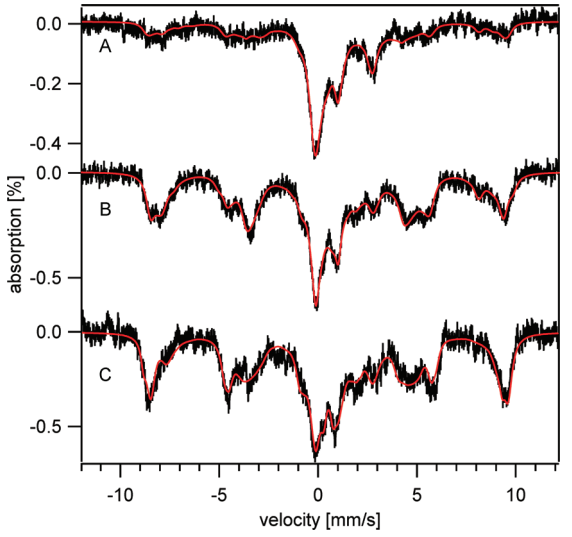

Figure 2. Mössbauer spectra of WT cells grown under various conditions. Spectra were collected at 6 K with 400 G magnetic field applied parallel to the γ-rays. (A−C) Cells grown on complete minimal medium containing 1, 40, and 500 μM ^{57}Fe(III) citrate, respectively. Red lines are simulations assuming the species and percentages listed in Table 3. Spectrum C was published previously as Figure 6A of ref 7.

μM Fe. When the Fe concentration of the growth medium was ≥40 μM, the iron concentration in Aft1-1^{up} cells only increased marginally (Table 2), perhaps reflecting saturation of the Aft1-dependent cellular iron uptake system.

Mössbauer Spectroscopy of Aft1-1^{up} Cells. We used Mössbauer spectroscopy to examine the Fe content of Aft1-1^{up} cells grown in medium containing different concentrations of Fe. With the limited resolution provided by Mössbauer spectroscopy, only a simplified analysis was possible. The four major types of features observed in Mössbauer spectra of Aft1-1^{up} (Figure 1) and WT cells (Figure 2) included (a) a six-line pattern between ca. −8 mm/s to +8 mm/s due to one or more mononuclear HS Fe(III) species, (b) a central quadrupole doublet due to $S = 0$ $[Fe_4S_4]^{2+}$ clusters and LS Fe(II) hemes, (c) a quadrupole doublet due to HS nonheme Fe(II) species, and (d) a broad partially resolved doublet due to Fe(III) (phosphate) nanoparticles. In spectra of isolated mitochondria, HS Fe(II) heme features can also be observed.[7] Parameters used to simulate these features are given in Table 3. Percentages of each feature in the displayed spectra are summarized in the lower part of the table. Previous analyses suggest that the HS Fe(III) species may arise from vacuoles,[3,7] and we will assume this here. Much of the remaining Fe species is located in mitochondria.[7]

Aft1-1^{up} cells grown in minimal medium supplemented with ~1 μM ^{57}Fe exhibited a 6 K Mössbauer spectrum (Figure 1A) containing significant amounts of HS Fe(III), whereas this feature in WT cells grown under similar conditions was substantially less intense (Figure 2A). The central and nonheme HS Fe(II) doublets in the WT spectrum were somewhat stronger than in the Aft1-1^{up} spectrum. The high energy line associated with the central doublet is at ~1 mm/s, while the low energy line is obscured by absorption centered near 0 mm/s. The high energy line of the nonheme HS Fe(II) doublet is at ~3.0 mm/s while the low energy line is also obscured by the absorption near 0 mm/s. No more than ~10% of the intensity of either spectrum was due to Fe(III) (phosphate) nanoparticles.

Given the presumed cellular location of the above-mentioned Fe species and the concentration of Fe in these cell types (Table 2), these differences in spectral intensities suggest that ~150 μM Fe in both Aft1-1^{up} and WT cells is associated with mitochondria while ~500 μM Fe in Aft1-1^{up} cells and 100 μM Fe in WT cells might be associated with vacuoles. These concentrations do not reflect the actual concentration of Fe in these

Table 3. Parameters Used for Mössbauer Spectral Simulations, Followed by Percentages of Component Species Associated with Spectra Indicated by Figure Number[a]

parameter	mononuclear nonheme HS Fe(III)[a]	central doublet[b]	nonheme HS Fe(II)[c]	Fe(III) (phosphate) nanoparticles[d]
δ (mm/s)	0.46 to 0.55	0.45	1.35	0.52
ΔE_Q (mm/s)	0.2 to 0.5	1.08	3.0	0.50
Γ (mm/s)	0.3 to 0.5	0.6	0.6	0.5
A_{iso} (kG)	−218 to −240			

Figure	%	%	%	%
1A	75	8	10	5
1B	70	7	5	12
1C	60	8	6	25
1D	58	8	8	22
1E	80	5	5	8
1F	70	5	7	14
2A	40	22	26	12
2B	73	5	10	12
2C	74	8	13	8
3A	<2	≤5	2	90
7A	65	20	10	6
7B	<2	5	12	76
7C	<2	≤2	5	88
7D	<2	≤5	5	90
7E	60	12	18	≤5

[a] Simulation of the HS Fe(III) features assumed three species, but this number is not physically meaningful, and the actual number of species contributing remains undetermined.

organelles ($[Fe]_{mito}$ or $[Fe]_{vac}$) but rather the product of the actual concentrations multiplied by the fractional volume of the organelle in the cell ($[Fe]_{mito}V_{mito}/V_{cell}$ and $[Fe]_{vac}V_{vac}/V_{cell}$, respectively). The concentration of Fe in isolated Aft1-1^{up} mitochondria (Table 2), along with this relationship, suggests that the mitochondria occupy ∼10% of the Aft1-1^{up} cellular volume. An important caveat is that these calculations rely on the cellular locations of the Mössbauer components. Our current assumption that all cellular Fe can be divided into mitochondrial and vacuolar locations[7] is undoubtedly an oversimplification.

It is interesting that the 3-fold reduction of the Aft1-dependent Fe regulon system in WT cells had no discernible impact on the amount of Fe associated with mitochondria. This suggests that the net rate of Fe entry into this organelle is insensitive to changes in the Aft1-dependent system, at least in cells grown with low $[Fe_{medium}]$. By net rate, we mean the import rate into the organelle minus the export rate. In contrast, the same fold reduction in the Aft1-dependent Fe regulon was associated with a 5-fold reduction of vacuolar Fe in WT cells. This suggests that the net import rate of Fe into vacuoles is Aft1-dependent.

The 6 K Mössbauer spectrum of Aft1-1^{up} cells grown on medium containing 5 μM ^{57}Fe also exhibited significant amounts of HS Fe(III) species (Figure 1B, Table 3). The percentage of cellular Fe in this form was diminished by ∼5%, relative to that in cells grown on 1 μM ^{57}Fe (Figure 1A). However, the overall percent effect increased substantially, which reflected the ∼3-fold increased concentration of Fe in Aft1-1^{up} cells grown on medium supplemented with 5 vs 1 μM ^{57}Fe (Table 2). In absolute amounts, the number of moles of Fe present as HS Fe(III) increased ∼3-fold in Aft1-1^{up} cells grown with 5 μM ^{57}Fe added to the medium vs the same cells grown with 1 μM ^{57}Fe added. This is consistent with an increased net rate of Fe import into the cell and an increased flow of Fe into vacuoles. Another important difference is that ∼12% of the intensity in the Mössbauer spectrum of the 5 μM ^{57}Fe-grown Aft1-1^{up} cells was due to Fe(III) (phosphate) nanoparticles. The same strain of cells, grown with 1 μM ^{57}Fe in the medium, was largely devoid of nanoparticles. We will show below that most (possibly all) of these nanoparticles are located in mitochondria. The formation of these particles reflects a greater import flow of Fe from the environment into these organelles.

These same trends continued for Aft1-1^{up} cells grown on medium supplemented with 40 μM ^{57}Fe (Figure 1C, Table 3). In these cells, the percentage of Fe due to HS Fe(III) was diminished relative to the Aft1-1^{up} sample grown on 5 μM added ^{57}Fe. However, the Fe content of the 40 μM Fe-grown Aft1-1^{up} cells was slightly higher (Table 2), such that the absolute amount of Fe present as HS Fe(III) actually increased, relative to the amount of HS Fe(III) in Aft1-1^{up} cells grown with 5 μM ^{57}Fe. This indicates an increased flow of Fe into the cell and perhaps into vacuoles as $[Fe_{medium}]$ increased. The relative intensity of nanoparticles also increased in the 40 μM Fe-grown Aft1-1^{up} cells, again suggesting an increased flow into mitochondria (see below). WT cells grown with 40 μM medium Fe also showed increased Fe levels associated with vacuoles, relative to WT cells grown on 1 μM ^{57}Fe (Figure 2B). Using the percentages given in Table 3 and the cellular Fe concentration given in Table 2, we conclude that ∼330 μM Fe was associated with vacuoles and ∼120 μM Fe with mitochondria in the WT cell grown with 40 μM ^{57}Fe. Only 12% of cellular Fe in these WT cells (∼50 μM) was present as nanoparticles, compared to 700 μM Fe as nanoparticles in Aft1-1^{up} cells. Thus, the extra mitochondrial

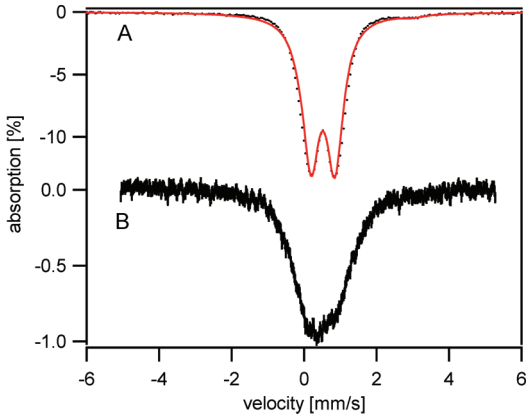

Figure 3. Mössbauer spectra of mitochondria isolated from Aft1-1^{up} cells grown on complete minimal medium containing 40 μM (A) and 1 μM Fe (B). The red line is a simulation assuming species and parameters listed in Table 3.

Fe beyond the ~150 μM mainly required for formation of respiratory complexes ultimately becomes nanoparticles.

The 6 K Mössbauer spectrum of Aft1-1^{up} cells grown on 500 μM ^{57}Fe (Figure 1D) was similar to that of the 40 μM ^{57}Fe-grown Aft1-1^{up} cells. The concentration of Fe in these cells was only slightly higher (Table 2), perhaps reflecting the saturation of the Aft1-dependent system. We conclude that the relative and absolute rates of Fe flowing into the cell, specifically into vacuoles and mitochondria, did not increase significantly in cells grown with 500 μM ^{57}Fe relative to cells grown with 40 μM ^{57}Fe. The spectrum exhibited by WT cells grown with 500 μM ^{57}Fe (Figure 2C) was quite similar to the WT sample grown with 40 μM ^{57}Fe. Although the Aft1 system is largely deactivated in WT cells at this [Fe$_{medium}$], the rate of Fe import from the environment appears to saturate under these conditions.

Mitochondria Isolated from Aft1-1^{up} Cells. To test whether the nanoparticles observed in Mössbauer spectra of Aft1-1^{up} cells grown with high [Fe$_{medium}$] were located in mitochondria, we isolated these organelles from Aft1-1^{up} cells grown on medium supplemented with 1 μM and with 40 μM ^{57}Fe. The Fe concentration of mitochondria from the 40 μM ^{57}Fe grown Aft1-1^{up} cells (Table 2) was ca. 11-fold higher than that reported for mitochondria isolated from WT cells grown under the same conditions.[27] The Fe concentration in mitochondria isolated from Aft1-1^{up} cells grown on 1 μM medium Fe was substantially reduced.

The 6 K Mössbauer spectrum of mitochondria isolated from Aft1-1^{up} cells grown with 40 μM ^{57}Fe (Figure 3A) was typical of Fe(III) (phosphate) nanoparticles.[11,12] These particles represented the vast majority of mitochondrial Fe. Also evident in the spectrum is the high energy line of a HS Fe(II) doublet. Although this doublet represented only a tiny percentage of the total intensity, the absolute concentration of the species represented by this feature was ~100 μM. Similar species, present at similar concentrations, have been reported for Yah1- and Atm1-depleted mitochondria.[11,12]

The 6 K Mössbauer spectrum of mitochondria isolated from Aft1-1^{up} cells grown on 1 μM ^{57}Fe was dominated by unresolved absorption at ~0.5 mm/s (Figure 3B). The percent effect was substantially reduced relative to the spectrum of mitochondria from cells grown on medium supplemented with 40 μM ^{57}Fe. As much as half of this intensity may be due to Fe(III) (phosphate) nanoparticles of the form displayed in Figure 3A. Other nanoparticle forms, or other unresolved features, could also be present. The spectrum of Figure 3B was readily contained within the corresponding whole-cell spectrum shown in Figure 1A, assuming ~5% of total intensity.

EPR spectroscopy provided further evidence for nanoparticles in mitochondria from Aft1-1^{up} cells grown on 40 μM medium Fe. Such organelles exhibited a broad peak around $g \sim 2$ with anti-Curie law behavior; i.e., the intensity of the peak increased as the sample temperature was raised from 10 K (Figure 4, top panel). Similar behavior was observed for Yah1p- and Atm1p-depleted mitochondria loaded with Fe(III) phosphate nanoparticles.[11,12]

Accumulation of Fe(III) phosphate nanoparticles in Yah1p- and Atm1p-depleted mitochondria is accompanied by elevated ROS damage.[11,12] An Oxyblot analysis was performed to determine whether accumulation of nanoparticles in Aft1-1^{up} mitochondria was also associated with increased ROS damage. Mitochondria isolated from two batches of WT cells, one grown on medium with 1 μM added Fe and the other grown with 40 μM added Fe, showed similar low levels of ROS damage (Figure 5, lanes A and B), consistent with the absence of substantial nanoparticles. In contrast, mitochondria isolated from Aft1-1^{up} cells grown under the same conditions exhibited elevated ROS damage (Figure 5, lanes C and D). Mitochondria from the Aft1-1^{up} cells grown with 40 μM ^{57}Fe had higher ROS damage, consistent with the increased amount of nanoparticles in samples prepared with that growth condition (Figure 1C) vs samples grown with 1 μM ^{57}Fe (Figure 1A).

We wondered whether this elevated ROS damage affected ISC and heme levels in Aft1-1^{up} mitochondria. Aconitase is a mitochondrial protein that requires an [Fe_4S_4] cluster for activity. Aconitase activities were essentially unchanged in mitochondria isolated from WT cells grown on medium containing 1 μM vs 40 μM Fe (780 units/mg of protein vs 850 units/mg of protein). In contrast, the aconitase activity was lower in mitochondria from Aft1-1^{up} cells grown with 40 μM added Fe than in organelles from cells grown with 1 μM added ^{57}Fe (Table 2). The activities of both growths of Aft1-1^{up} cells were lower relative to their WT controls. This indicates that ISC levels declined when nanoparticles accumulated in mitochondria.

Further evidence for a nanoparticle-associated decline of ISCs comes from EPR spectroscopy. The $g \sim 1.94$ signal, which arises from reduced ISCs, was weaker in spectra of mitochondria isolated from cells grown on 40 μM medium Fe than in mitochondria from cells grown with 1 μM Fe (Figure 4, bottom panel). Heme levels were also decreased in Aft1-1^{up} cells relative to WT cells, even at 1 μM medium Fe concentration (Figure 6). The decline in ISC and heme levels is probably due to degradation caused by the ROS damage that accompanies Fe accumulation, as we have proposed previously for Atm1p-depleted mitochondria.[11]

Media Dependence of Nanoparticles. Aft1-1^{up} cells grown in standard rich medium (YPGal), as well as the mitochondria isolated from such cells, reportedly do not accumulate Fe.[20] In minimal medium, a similar Fe concentration caused substantial Fe nanoparticle buildup in Aft1-1^{up} cells and mitochondria (Figure 1B,C). We wondered whether this difference arose from differences in the medium used to grow the cells. Without adding Fe, rich medium contained ~20 μM Fe. When 20 μM ^{57}Fe was added to standard YPD medium (giving a total [Fe] of ~40 μM), the resulting spectrum (Figure 1E) did not contain a significant amount of the Fe(III) (phosphate) nanoparticle doublet. In YPD medium, noticeable nanoparticles formed in cells grown on very high media Fe concentration (e.g., 400 μM medium Fe,

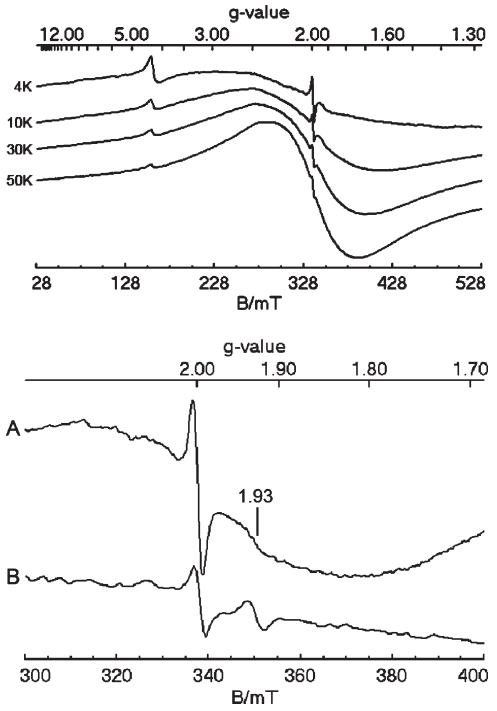

Figure 4. EPR spectra of the mitochondria isolated from Aft1-1^{up} cells. Top panel: Mitochondria from cells grown on 40 μM Fe, recorded at 20 mW microwave power, 9.46 GHz, and 4, 10, 30, and 50 K, respectively. Bottom panel: Mitochondria from cells grown on 40 μM (A) and 1 μM (B) Fe, recorded at 0.2 mW microwave power, 9.46 GHz, and 10 K.

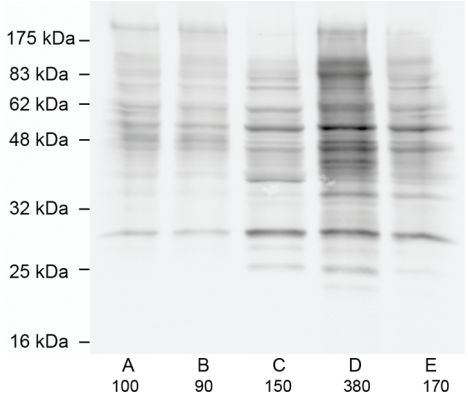

Figure 5. Oxyblot analysis of WT and Aft1-1^{up} mitochondria. Lanes A and B, mitochondria isolated from WT cells grown on complete minimal medium supplemented with 1 and 40 μM ^{57}Fe, respectively; lanes C and D, mitochondria isolated from Aft1-1^{up} cells grown on complete minimal medium supplemented with 1 and 40 μM ^{57}Fe, respectively; lane E, mitochondria isolated from Aft1-1^{up} cells grown on YPD medium supplemented with 20 μM ^{57}Fe. The sum of the band intensities of each lane was normalized to that of lane A. Relative percentages are given at the bottom of the figure.

Figure 1F). The extent of nanoparticle buildup with 40 μM Fe in YPD medium was similar to that for cells grown on minimal medium supplemented with 1 μM ^{57}Fe (Figure 1A). Moreover, the extent of oxidative damage for these two conditions was similar (compare Figure 5C vs Figure 5E). Supplementing YPD medium with 400 μM ^{57}Fe (Figure 1F) resulted in about the same level of nanoparticles as was obtained by supplementing

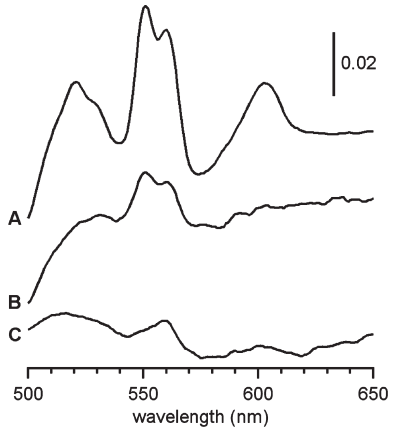

Figure 6. UV−vis spectra of mitochondria isolated from WT and Aft1-1^{up} cells grown on minimal media. (A) Mitochondria from WT cells grown with 20 μM ^{57}Fe. (B) Mitochondria from Aft1-1^{up} cells grown with 1 μM ^{57}Fe. (C) Mitochondria from Aft1-1^{up} cells grown with 40 μM ^{57}Fe.

minimal medium with 5 μM ^{57}Fe (Figure 1B). YPD has additional nutrients relative to minimal medium, which might allow cells to adjust more flexibly to the Aft1-1^{up}-induced perturbation. Alternatively, the magnitude of this perturbation may be attenuated in YPD-grown cells.

Vacuolar Fe in Aft1-1^{up} vs Yah1p-Depleted Cells. We have reported previously that disruption of mitochondrial ISC assembly causes a dramatic shift in cellular iron distribution.[11] This shift is thought to arise because yeast cells depleted in proteins associated with ISC assembly (e.g., Yah1p, Atm1p, Yfh1p) "feel" Fe-deficient and thus upregulate expression of Aft1-targeted genes, similar to the expression level situation in Aft1-1^{up} cells.[28] This suggested that the cellular distribution of Fe in Yah1p- and Atm1p-depleted (and perhaps Yfh1p-depleted) cells should be similar to that of Aft1-1^{up} cells.

To test this idea, we examined the Fe distribution in whole Yah1p-deficient cells. Gal-YAH1 cells were cultured in complete minimal medium containing galactose. In the presence of galactose, these cells express Yah1p. The resulting Mössbauer spectrum (Figure 7A) was typical of WT cells. Aliquots of this culture were diluted into fresh minimal medium containing glucose as carbon source and were allowed to grow for an additional 12 and 18 h. Under these conditions YAH1 was repressed (Figure 7, upper panel). After 12 h of growth, cells were harvested and examined by Mössbauer spectroscopy. The 6 K spectrum (Figure 7B) was dominated by a nanoparticle doublet. The remaining ~5% of spectral intensity was a high-spin Fe(II) doublet, with no evidence of mononuclear HS Fe(III) species. Thus, virtually all cellular Fe in Yah1p-depleted cells was present as nanoparticles. In another similar experiment, Yah1p-depleted cells were harvested after an additional 18 h of growth. The 6 K Mössbauer spectrum of these cells (Figure 7C) was similar to Figure 7B, except that the percent effect due to the nanoparticles had increased. The percentage of the HS Fe(II) form decreased, but the absolute concentration of the HS Fe(II) species probably remained about the same. When Gal-YAH1 cells were grown on low Fe medium (1 μM ^{57}Fe added), the dominant cellular Fe form was still Fe(III) nanoparticles (Figure 7D).

Comparing these spectra to those of Aft1-1^{up} cells (Figure 1, A-F) reveals that ~70% of the Fe in Aft1-1^{up} cells was present as

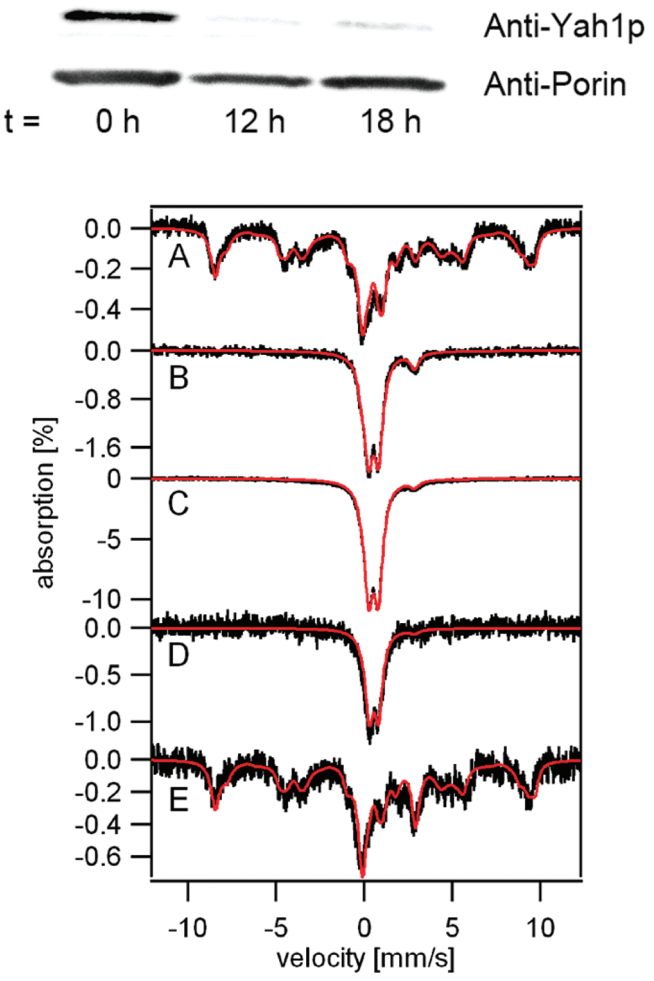

Figure 7. Western blot and Mössbauer spectra of Gal-YAH1 and Aft2-1^{up} cells. Gal-YAH1 cells were cultured in complete minimal medium supplemented with 40 μM ^{57}Fe and containing galactose. When OD (600 nm) reached ~1, cells were harvested, and a portion was used for Western blot, crude mitochondria isolation, and whole-cell Mössbauer spectroscopy. The remaining cells were diluted at t = 0 into fresh minimal medium containing glucose as carbon source. At t = 12 and 18 h, these cells were harvested, mitochondria were isolated, and whole-cell Mössbauer samples were prepared. Top panel: Western blot of crude mitochondria showing Yah1p and porin (loading control) expression levels. Bottom panel: 6 K Mössbauer spectra of (A) Gal-YAH1 cells grown in galactose-containing medium; (B) Gal-YAH1 cells after switching to glucose-containing medium and harvesting at 12 h; (C) same as (B) but cells were harvested at 18 h; (D) Gal-YAH1 cells grown on minimal glucose medium supplemented with 1 μM ^{57}Fe for ~18 h (final OD (600 nm) ~ 1); (E) Aft2-1^{up} cells grown on minimal glucose medium supplemented with 40 μM ^{57}Fe. Red lines are simulations assuming the species and percentages listed in Table 3.

HS Fe(III) species, probably located in vacuoles, whereas little, if any, Fe in Yah1-depleted cells is of this form. Both cells contained significant amounts of Fe(III) (phosphate) nanoparticles. Previous studies have shown that such nanoparticles are found in mitochondria of Yah1p-depleted cells.[12] Our current study indicates the same for the mitochondria of Aft1-1^{up} cells, but only when cells were grown in medium containing Fe at high concentrations. We believe that essentially all nanoparticles in Aft1-1^{up}, Yah1-depleted, and Atm1-depleted cells are located in mitochondria. We cannot exclude the possibility that a small portion is located in other cellular compartments (e.g., cytosol, vacuoles), but neither do we have evidence for this.

Distribution of Iron in Aft2-1^{up} Cells. In the Aft2-1^{up} strain, Aft2-targeted genes are constitutively activated, analogous to the condition in Aft1-1^{up} cells.[22] Microarray data suggest that Aft2-targeted genes may be involved in intracellular Fe trafficking.[29] Aft2p activates the vacuolar iron exporter Smf3p and the mitochondrial Fe importers Mrs3p/Mrs4p; thus, Aft2p is suspected of promoting Fe transport from vacuoles to mitochondria. In this case, activation of Aft2p-controlled genes would be expected to deplete vacuoles of Fe and cause Fe to accumulate in mitochondria, as observed in Yahp1-depleted cells but not in Aft1-1^{up} cells. The Mössbauer spectrum of Aft2-1^{up} cells (in a $\Delta aft1$ background) grown on medium with 40 μM ^{57}Fe (Figure 7D) was similar to that of WT cells, including a significant amount of HS Fe(III) species and central doublet. This similarity suggests that activation of Aft2p-targeted genes does not significantly alter cellular iron distribution.

DISCUSSION

The primary objective of this study was to better understand the regulation of cellular Fe by Aft1p and the iron regulon. We used an integrative biophysical approach to study the Aft1-1^{up} strain grown in medium containing different concentrations of ^{57}Fe. We wanted to determine how the cellular Fe arising from Aft1p-dependent import was distributed in the cell and to compare this distribution to those obtained using WT and Yah1-depleted cells. On the basis of these results, we developed a model (Figure 8) to interpret the observed changes in Fe distribution. Shown are approximate concentrations of various types of Fe present in fermenting WT, Aft1-1^{up}, and Yah1p-depleted cells grown in Fe-deficient minimal media supplemented with low and high iron.

Effect of Media Fe on Cellular Fe Distribution. Under low Fe growth conditions, Aft1-1^{up} cells contained more Fe than WT cells, and that Fe was distributed somewhat differently. Most of the Fe in Aft1-1^{up} cells was mononuclear nonheme HS Fe(III) species, assumed to be located in vacuoles. WT cells contained HS Fe(III) species, but in lesser amounts. Yah1p-depleted cells did not contain such species. In Aft1-1^{up} cells, a substantial portion of Fe was in the form of ISC and heme prosthetic groups, most of which was located in mitochondria. Similar concentrations of ISCs and hemes were present in WT cells grown under similar conditions. Yah1p-depleted cells were essentially devoid of these prosthetic groups; the vast majority of the Fe in these cells was present as Fe(III) phosphate nanoparticles. A small portion of Fe in Aft1-1^{up} cells was also nanoparticles, whereas these particles were less evident in comparably grown WT cells.

As the concentration of ^{57}Fe in the medium of Aft1-1^{up} cells increased, the most significant change was an increase of cellular Fe that was not matched in WT cells. The difference in cellular Fe concentrations was probably due to the constitutive upregulation of Fe importers on the plasma membrane in Aft1-1^{up} cells vs the Fe-dependent shutdown of these importers in WT cells. These results suggest that the concentration of cytosolic Fe species, or at least that particular species that is sensed by the Aft1 system, is proportional to [Fe_{medium}] in this range of concentrations..

In Aft1-1^{up} cells, some of the additional Fe was delivered to vacuoles and some to mitochondria, such that the percentage of Fe in the two organelles did not dramatically change relative to the low-Fe growth condition. Mitochondria from WT cells had a substantial amount of Fe present in respiration-related prosthetic

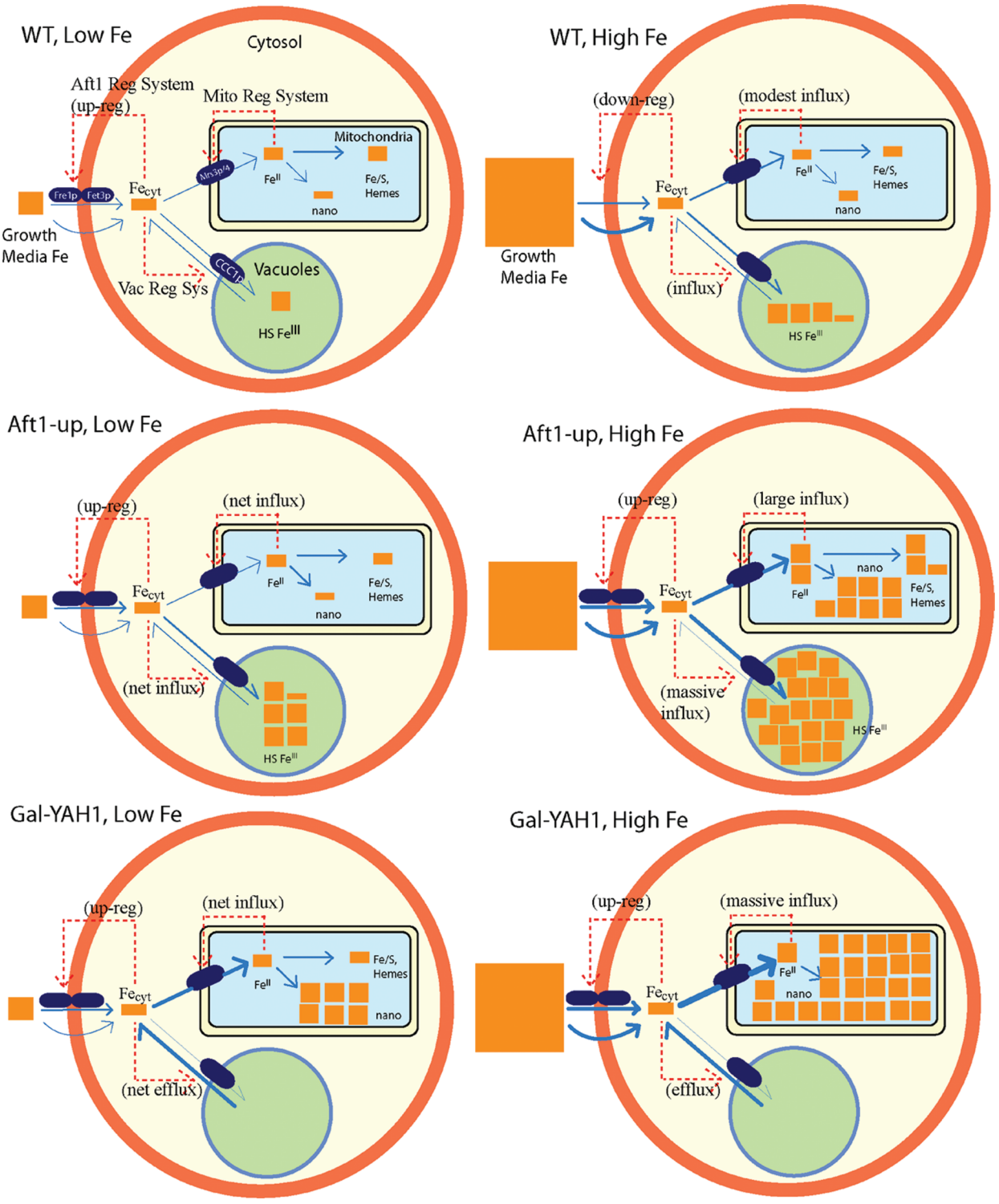

Figure 8. Model of cellular iron distribution in WT, Aft1-1^{up}, and Gal-YAH1 cells grown on low (~1 μM) and high (≥40 μM) iron. In WT cells grown in low [Fe_{medium}], the iron regulon is partially activated. Imported Fe is delivered primarily to the mitochondria, where much of it is assembled into Fe/S clusters and heme centers. Some Fe is sent to vacuoles, where it resides in the HS Fe(III) state. When WT cells are grown in high [Fe_{medium}], Aft1 is downregulated, shifting the burden of importing Fe to Aft1-independent pathways (curved blue arrows). In Aft1-1^{up} cells, Aft1 is constitutively activating the iron regulon regardless of the concentration of Fe_{medium}. When grown in low [Fe_{medium}], more Fe is imported relative to WT cells. The majority is sent to vacuoles while much of the remainder is sent to mitochondria for heme and ISC biosynthesis. When Aft1-1^{up} cells are grown in high [Fe_{medium}], the rate of import is increased, but the imported Fe is distributed similarly. The flow into mitochondria is favored because nanoparticle formation depresses the concentration of the precursor Fe species in the matrix that is both sensed for regulation and converted into nanoparticles. Mitochondria "feel" Fe-deficient, accelerating Fe import. In Yah1p-depleted cells grown at either low or high media Fe, nearly all imported Fe is delivered to mitochondria. This massive influx of Fe into the mitochondria depresses the concentration of cytosolic Fe that is sensed by the Aft1 regulatory system and by the vacuolar iron regulatory system (Fe_{cyt}). Due to this regulatory structure, these cells "feel" Fe deficient, leading to an increased import of Fe_{medium} and the efflux of Fe from the vacuole, as the regulatory system attempts to increase Fe_{cyt}.

dx.doi.org/10.1021/bi102015s |*Biochemistry* 2011, 50, 2660–2671

groups and a comparable amount of Fe(III) (phosphate) nanoparticles (and perhaps some mononuclear HS Fe(III)[7]). In contrast, the Fe in mitochondria from Aft1-1^{up} cells was predominantly in the form of Fe(III) (phosphate) nanoparticles.

Aft1-1^{up} cells grown with very high media Fe contained marginally more Fe than when grown on intermediate Fe levels. The fractional increase was modest relative to the increase in cellular Fe when [Fe_{medium}] was increased from low to intermediate levels. This suggests that the Aft1-dependent rate of Fe import into the cell saturates at high [Fe_{medium}]. A disproportionate amount of the additional Fe was imported into mitochondria, where it formed Fe(III) (phosphate) nanoparticles. Yah1-depleted cells also accumulated such nanoparticles.

Nanoparticle Formation. Fe(III) (phosphate) nanoparticles formed in the mitochondria of all three cell types examined, with more nanoparticles formed when cells were grown in media supplemented with high concentrations of Fe. The greatest accumulation of nanoparticles was observed with Yah1p-depleted cells, followed by Aft1-1^{up} cells and then WT cells. Under nanoparticle forming conditions, there was a massive influx of iron (presumably HS Fe(II)) into the mitochondrial matrix. This was probably followed by oxidation to Fe(III), ligand exchange to include phosphate ions in the coordination sphere, and then precipitation as Fe(III) phosphate nanoparticles. Why the mitochondria in these cells are so conducive to nanoparticle formation is unclear, but possibilities include an increase in the concentration of matrix Fe beyond its solubility limit, an unusually oxidizing matrix environment, a higher than normal pH, and an altered chemical composition of the matrix.

ISCs and heme levels are diminished in Aft1-1^{up} mitochondria when cells are grown under nanoparticle-forming conditions. Nanoparticle formation was strongly correlated to ROS production. Similar to the situation with Yah1p-depleted[12] and Atm1-depleted[11] cells, we suggest that ISCs and heme centers are being biosynthesized in Aft1-1^{up} cells but that these centers are destroyed by ROS generated during nanoparticle formation.

Similar ISC and heme defects have been noted for numerous other mitochondrial proteins that are thought to be involved in the pathways that biosynthesize these centers. Interestingly, there is no direct disruption of these biosynthesis pathways in Aft1-1^{up} cells, and microarray studies have shown that proteins associated with these pathways are not downregulated.[22] The fact that ISC and heme levels are diminished by mutating Aft1p, *a protein that never enters the mitochondria* and is only indirectly involved in these pathways, highlights the possibility that the commonly observed ISC and heme depletion phenotype is a secondary effect due to ROS damage. Diminished ISCs or heme centers should not be automatically interpreted as demonstrating the primary functions of the proteins whose deletion causes these effects.

Cytosolic Fe. We could not unambiguously discern, based on our results, cytosolic Fe with any cell type or under any growth condition. We suspect that some cytosolic Fe is present as nonheme HS Fe(II) species. If so, the spectral intensities associated with these species (Table 3) represent the upper limit for the cytosolic Fe pool. For example, the spectrum of Figure 1A indicates that the cytosolic Fe in Aft1-1^{up} cells grown on low Fe can be no more than ~10% of cellular Fe, corresponding to ~65 μM HS Fe(II) species. Some of this Fe is probably in other cellular locations, e.g., in the mitochondria. Other types of Fe may be found in the cytosol. In the same spectrum, the central doublet represents ~8% of total intensity. The majority of this doublet arises from $S = 0$ $[Fe_4S_4]^{2+}$ clusters, suggesting a maximum cellular concentration of ~14 μM for such clusters. A majority of these clusters are undoubtedly in mitochondria, but some may be cytosolic. The cytosol may also contain mononuclear HS Fe(III) species, but because so much cellular HS Fe(III) is observed by Mössbauer, and some or all of this Fe may be located in vacuoles, the cytosolic contribution cannot be estimated reliably.

Aft1p-Dependent Regulation. We have developed a simple Fe regulatory model (red dashed lines in Figure 8) to explain our results. The general characteristics of homeostatic regulatory systems are well understood.[30,31] Such systems include a molecule whose concentration is sensed, a mechanism for comparing this concentration to a set-point concentration, and a mechanism for adjusting the concentration of the sensed molecule toward the set-point value. In some systems, including Aft1, regulation is at the genetic level, involving transcription factors and control of gene expression. In other systems, regulation is at the protein level, involving allosterically regulating protein activities.

In our model, we do not consider whether a particular regulation system operates at the genetic or protein level, nor do we consider what particular form of Fe is being sensed or the particular proteins involved. Rather, we consider the minimum number of Fe regulatory systems that might be involved, the cellular locations of the sensed molecules and responding proteins, the cellular compartments across which Fe moves, and the particular types of Fe species that move. We limit considerations to three cellular compartments, namely, the cytosol, vacuole, and mitochondria.

The Aft1 system regulates the import of Fe from the environment into the cytosol.[4] It undoubtedly senses the concentration of a cytosolic Fe species (Fe_{cyt}). In WT cells, the Aft1 system is deactivated at [Fe_{medium}] > low micromolar; at 40 μM, the system is significantly attenuated. Thus, there are other pathways by which Fe enters the cell. These become increasingly important as the Aft1 system is shut down, but they saturate when [Fe_{medium}] > ~40 μM. The Aft1-dependent iron regulon is upregulated in Atm1-depleted and Yah1p-depleted cells; i.e., such cells "feel" as though they are Fe-deficient.

Whether the Aft1 system also regulates the trafficking of cytosolic Fe into vacuoles and mitochondria is unknown, but we suggest that it does not. We propose that there are (at least) two additional Fe homeostatic regulatory mechanisms in yeast, one that regulates the influx and efflux of vacuolar Fe and one that regulates the influx of mitochondrial Fe. The Aft1 system influences these other systems through the effects of sharing a common pool of cytosolic Fe, namely, Fe_{cyt}. As Fe from the environment enters the cytosol and [Fe_{cyt}] increases, the influx of Fe into these organelles will also increase by simple mass action kinetics.

Vacuolar Iron Regulatory System. The main difference in Fe contents between Aft1-1^{up} cells and Yah1p-depleted cells is that Aft1-1^{up} cells contain a significant amount of what appears to be vacuolar Fe while Yah1p-depleted cells are devoid of the presumed vacuolar Fe, regardless of [Fe_{medium}]. Vacuoles likely function as reservoirs for storing and releasing Fe. Thus, Yah1p-depleted cells may "feel" Fe-deficient, even when grown in Fe-replete media, and they respond by expelling Fe from the vacuoles. In contrast, Aft1-1^{up} cells "feel" Fe sufficient (except perhaps at very low [Fe_{medium}]), and they respond by importing Fe into the vacuole.

We propose that the fluxes of Fe into and out of vacuoles are regulated by an Aft1-independent regulatory system that senses

[Fe_{cyt}]. Accordingly, the steady-state concentration of [Fe_{cyt}] in Yah1p-depleted cells would be predicted to be lower than in Aft1-1^{up} and WT cells, explaining why Yah1p-depleted vacuoles are devoid of Fe and why they are filled in Aft1-1^{up} cells. The set-point concentration of [Fe_{cyt}] is probably somewhere between these concentrations. Regulation could be at the transcriptional level, in that the expression of such transporters could be sensitive to these relationships. This could explain why in Yah1p- and Atm1p-depleted cells the vacuolar importer CCC1 is transcriptionally repressed and the vacuolar exporter complex FET5/FTH1 is upregulated (see Supporting Information of ref 28). Expression of these genes is *not* controlled by Aft1, suggesting a different regulatory system. Yap5p regulates CCC1 expression in an Fe-dependent manner, and it should be viewed as a candidate for this regulatory system.[32]

Mitochondrial Iron Regulatory System. Another difference between Aft1-1^{up} and Yah1p-depleted cells is that nearly all of the Fe in Yah1p-depleted cells is present as Fe(III) (phosphate) nanoparticles located in mitochondria. Aft1-1^{up} mitochondria also contain nanoparticles, but in lesser amounts. If mitochondria and vacuoles imported cytosolic Fe from the same pool and sensed the same Fe_{cyt} species, this could explain why Fe accumulates in both mitochondria and vacuoles of Aft1-1^{up} cells, namely, because [Fe_{cyt}] exceeds its set-point concentration. However, this same reasoning cannot explain why Fe accumulates in Yah1p-depleted mitochondria but is expelled from their vacuoles. This leads us to propose that mitochondria contain a separate regulatory system similar to that previously proposed for Yah1p-depleted cells.[12] The rate of Fe import into mitochondria was proposed to be controlled by the concentration of an Fe species in the matrix, Fe_{matrix}, that is eventually converted into nanoparticles. Nanoparticle formation would depress [Fe_{matrix}], causing the system to import more Fe from the cytosol as the homeostatic regulatory response. Since the amount of precipitated nanoparticles in the matrix is not sensed, the regulatory system never reduces the Fe import rate. Regulation could be at the local level (activating existing Fe importers on the mitochondrial IM) or at the genetic level (upregulating the biosynthesis of more Fe importers). In the latter case, the status of Fe in the matrix would somehow need to be communicated to the nucleus where gene expression levels are controlled. Lill has suggested that the IM protein Atm1p exports such a sensor.[1]

Further studies are required to establish the existence of these two proposed regulatory systems and to explore the molecular level details of how they function. Central to this effort will be to identify cytosolic and matrix Fe species that might serve as sensors for these systems.

■ ASSOCIATED CONTENT

Supporting Information. The primer pairs used for the RT-PCR experiment (Table S1) and fluorescence data used to determine void volumes in cell pellets (Table S2). This material is available free of charge via the Internet at http://pubs.acs.org.

■ AUTHOR INFORMATION

Corresponding Author

*Phone: 979-845-0956. Fax: 979-845-4719. E-mail: lindahl@chem.tamu.edu.

Funding Sources

This study was supported by the National Institutes of Health (GM084266) and the Robert A. Welch Foundation (A1170).

■ ACKNOWLEDGMENT

We thank Drs. Jerry Kaplan, Roland Lill, and Dennis Winge for providing the genetic strains of yeast used in this study, Kevin Burgess for providing the fluorescent Compound 5, Ryland Young for use of his fluorescence spectrometer, and Laurie Davidson for help in designing and performing the RT-PCR.

■ ABBREVIATIONS

Fe_{medium}, iron contained in the growth medium; Aft1-1^{up}, a yeast strain in which the transcription factor Aft1p constitutively upregulates iron regulon genes, regardless of Fe_{medium} concentration; Aft2-1^{up}, similar to Aft1-1^{up} but for the gene Aft2; GalYAH1, a yeast strain in which expression of the ferredoxin Yah1 is controlled by the carbon source in the growth medium (galactose promotes expression; glucose represses it); WT, wild type; ND, not determined; ISC, iron−sulfur cluster; Ccc1p, Fe importer on the vacuolar membrane; IM, inner membrane of the mitochondria; Mrs3p and Mrs4p, Fe importers on the IM; ROS, reactive oxygen species; YPD, standard rich medium containing glucose; BPS, bathophenanthrolinesulfonate; Compound 5, a fluorescent compound described in ref 25; δ, isomer shift; ΔE_Q, quadrupole splitting; HS, high spin; LS, low spin; EPR, electron paramagnetic resonance; Fe_{cyt}, unidentified Fe in the cytosol sensed by the Aft1 regulatory system; Fe_{matrix}, unidentified Fe in the mitochondrial matrix that is proposed to be sensed by the mitochondrial iron regulatory system.

■ ADDITIONAL NOTE

[a]Throughout this paper, we place "phosphate" in parentheses when referring to Fe(III) (phosphate) nanoparticles in Aft1-1^{up} cells because we presume, but have not demonstrated, that they contain phosphate groups. Phosphate is associated with nanoparticles in Atm1p-deficient and Yfh1-deficient mitochondria.[10,11,13] Mössbauer spectra of Aft1-1^{up} nanoparticles are nearly indistinguishable from those of Atm1p-deficient cells.

■ REFERENCES

(1) Lill, R. (2009) Function and biogenesis of iron-sulphur proteins. *Nature 460*, 831–838.

(2) Eide, D., Daviskaplan, S., Jordan, I., Sipe, D., and Kaplan, J. (1992) Regulation of iron uptake in *Saccharomyces cerevisiae*—the ferrireductase and Fe(II) transporter are regulated independently. *J. Biol. Chem. 267*, 20774–20781.

(3) Kosman, D. J. (2003) Molecular mechanisms of iron uptake in fungi. *Mol. Microbiol. 47*, 1185–1197.

(4) Yamaguchi-Iwai, Y., Ueta, R., Fukunaka, A., and Sasaki, R. (2002) Subcellular localization of Aft1 transcription factor responds to iron status in *Saccharomyces cerevisiae*. *J. Biol. Chem. 277*, 18914–18918.

(5) Li, H. R., Mapolelo, D. T., Dingra, N. N., Naik, S. G., Lees, N. S., Hoffman, B. M., Riggs-Gelasco, P. J., Huynh, B. H., Johnson, M. K., and Outten, C. E. (2009) The yeast iron regulatory proteins Grx3/4 and Fra2 form heterodimeric complexes containing a [2Fe-2S] cluster with cysteinyl and histidyl ligation. *Biochemistry 48*, 9569–9581.

(6) Yamaguchiiwai, Y., Dancis, A., and Klausner, R. D. (1995) Aft1—a mediator of iron-regulated transcriptional control in *Saccharomyces cerevisiae*. *EMBO J. 14*, 1231–1239.

(7) Holmes-Hampton, G. P., Miao, R., Morales, J. G., Guo, Y. S., Münck, E., and Lindahl, P. A. (2010) A nonheme high-spin ferrous pool

in mitochondria isolated from fermenting *Saccharomyces cerevisiae*. *Biochemistry 49*, 4227–4234.

(8) Tsai, C. L., and Barondeau, D. P. (2010) Human frataxin is an allosteric switch that activates the Fe-S cluster biosynthetic complex. *Biochemistry 49*, 9132–9139.

(9) Lesuisse, E., Santos, R., Matzanke, B. F., Knight, S. A. B., Camadro, J. M., and Dancis, A. (2003) Iron use for haeme synthesis is under control of the yeast frataxin homologue (Yfh1). *Hum. Mol. Genet. 12*, 879–889.

(10) Seguin, A., Santos, R., Pain, D., Dancis, A., Camadro, J.-M., and Lesuisse, E. Co-precipitation of phosphate and iron limits mitochondrial phosphate availability in *Saccharomyces cerevisiae* lacking the yeast frataxin homologue (YFH1), *J. Biol. Chem.* (in press).

(11) Miao, R., Kim, H., Koppolu, U. M. K., Ellis, E. A., Scott, R. A., and Lindahl, P. A. (2009) Biophysical characterization of the iron in mitochondria from Atm1p-depleted *Saccharomyces cerevisiae*. *Biochemistry 48*, 9556–9568.

(12) Miao, R., Martinho, M., Morales, J. G., Kim, H., Ellis, E. A., Lill, R., Hendrich, M. P., Münck, E., and Lindahl, P. A. (2008) EPR and Mössbauer spectroscopy of intact mitochondria isolated from Yah1p-depleted *Saccharomyces cerevisiae*. *Biochemistry 47*, 9888–9899.

(13) He, W., Zhou, W. J., Wang, Y. J., Zhang, X. D., Zhao, H. S., Li, Z. M., and Yan, S. P. (2009) Biomineralization of iron phosphate nanoparticles in yeast cells. *Mater. Sci. Eng., C 29*, 1348–1350.

(14) Li, L. T., Chen, O. S., Ward, D. M., and Kaplan, J. (2001) CCC1 is a transporter that mediates vacuolar iron storage in yeast. *J. Biol. Chem. 276*, 29515–29519.

(15) Singh, A., Kaur, N., and Kosman, D. J. (2007) The metalloreductase Fre6p in Fe-Efflux from the yeast vacuole. *J. Biol. Chem. 282*, 28619–28626.

(16) Li, L. T., and Kaplan, J. (2004) A mitochondrial-vacuolar signaling pathway in yeast that affects iron and copper metabolism. *J. Biol. Chem. 279*, 33653–33661.

(17) Foury, F., and Roganti, T. (2002) Deletion of the mitochondrial carrier genes MRS3 and MRS4 suppresses mitochondrial iron accumulation in a yeast frataxin-deficient strain. *J. Biol. Chem. 277*, 24475–24483.

(18) Chen, O. S., and Kaplan, J. (2000) CCC1 suppresses mitochondrial damage in the yeast model of Friedreich's ataxia by limiting mitochondrial iron accumulation. *J. Biol. Chem. 275*, 7626–7632.

(19) Mühlenhoff, U., Stadler, J. A., Richhardt, N., Seubert, A., Eickhorst, T., Schweyen, R. J., Lill, R., and Wiesenberger, G. (2003) A specific role of the yeast mitochondrial carriers Mrs3/4p in mitochondrial iron acquisition under iron-limiting conditions. *J. Biol. Chem. 278*, 40612–40620.

(20) Babcock, M., deSilva, D., Oaks, R., DavisKaplan, S., Jiralerspong, S., Montermini, L., Pandolfo, M., and Kaplan, J. (1997) Regulation of mitochondrial iron accumulation by Yfh1p, a putative homolog of frataxin. *Science 276*, 1709–1712.

(21) Lange, H., Kaut, A., Kispal, G., and Lill, R. (2000) A mitochondrial ferredoxin is essential for biogenesis of cellular iron-sulfur proteins. *Proc. Natl. Acad. Sci. U.S.A. 97*, 1050–1055.

(22) Rutherford, J. C., Jaron, S., and Winge, D. R. (2003) Aft1p and Aft2p mediate iron-responsive gene expression in yeast through related promoter elements. *J. Biol. Chem. 278*, 27636–27643.

(23) Lindahl, P. A., Morales, J. G., Miao, R., and Holmes-Hampton, G. (2009) Isolation of *Saccharomyces cerevisiae* mitochondria for Mössbauer, EPR, and electronic absorption spectroscopic analyses. *Method Enzymol. 456*, 267–285.

(24) Schmitt, M. E., Brown, T. A., and Trumpower, B. L. (1990) A rapid and simple method for preparation of RNA from *Saccharomyces cerevisiae*. *Nucleic Acids Res. 18*, 3091–3092.

(25) Jose, J., Loudet, A., Ueno, Y., Barhoumi, R., Burghardt, R. C., and Burgess, K. (2010) Intracellular imaging of organelles with new water-soluble benzophenoxazine dyes. *Org. Biomol. Chem. 8*, 2052–2059.

(26) Hudder, B. N., Morales, J. G., Stubna, A., Münck, E., Hendrich, M. P., and Lindahl, P. A. (2007) Electron paramagnetic resonance and Mössbauer spectroscopy of intact mitochondria from respiring *Saccharomyces cerevisiae*. *J. Biol. Inorg. Chem. 12*, 1029–1053.

(27) Morales, J. G., Holmes-Hampton, G. P., Miao, R., Guo, Y. S., Münck, E., and Lindahl, P. A. (2010) Biophysical characterization of iron in mitochondria isolated from respiring and fermenting yeast. *Biochemistry 49*, 5436–5444.

(28) Hausmann, A., Samans, B., Lill, R., and Mühlenhoff, U. (2008) Cellular and mitochondrial remodeling upon defects in iron-sulfur protein biogenesis. *J. Biol. Chem. 283*, 8318–8330.

(29) Courel, M., Lallet, S., Camadro, J. M., and Blaiseau, P. L. (2005) Direct activation of genes involved in intracellular iron use by the yeast iron-responsive transcription factor Aft2 without its paralog Aft1. *Mol. Cell. Biol. 25*, 6760–6771.

(30) Sewell, C., Morgan, J. J., and Lindahl, P. A. (2002) Analysis of protein homeostatic regulatory mechanisms in perturbed environments at steady state. *J. Theor. Biol. 215*, 151–167.

(31) Yang, Q. W., Lindahl, P. A., and Morgan, J. J. (2003) Dynamic responses of protein homeostatic regulatory mechanisms to perturbations from steady state. *J. Theor. Biol. 222*, 407–423.

(32) Li, L., Bagley, D., Ward, D. A., and Kaplan, J. (2008) Yap5 is an iron-responsive transcriptional activator that regulates vacuolar iron storage in yeast. *Mol. Cell. Biol. 28*, 1326–1337.